Low dielectric loss $BaNd_2Ti_5O_{14}$ thick films prepared by an electrophoretic deposition technique

Zhi Fu, Aiying Wu, P. M. Vilarinho, A. I. Kingon, and R. Wördenweber

Citation: Appl. Phys. Lett. **90**, 052912 (2007); doi: 10.1063/1.2435334
View online: https://doi.org/10.1063/1.2435334
View Table of Contents: http://aip.scitation.org/toc/apl/90/5
Published by the American Institute of Physics

Low dielectric loss $BaNd_2Ti_5O_{14}$ thick films prepared by an electrophoretic deposition technique

Zhi Fu, Aiying Wu, and P. M. Vilarinho[a)]
Department of Ceramics and Glass Engineering, CICECO, University of Aveiro, 3810-193 Aveiro, Portugal

A. I. Kingon
Materials Research Center, North Carolina State University, Raleigh, North Carolina 27695-7919

R. Wördenweber
Division Superconductivity and High Frequency Sensors, Institute of Thin-films and Interfaces, Forschungszentrum Jülich GmbH, 52425 Jülich, Germany

(Received 16 July 2006; accepted 27 December 2006; published online 2 February 2007)

$BaNd_2Ti_5O_{14}$ (BNT) films 12–52 μm thick were fabricated on platinum metallic foils by electrophoretic deposition (EPD). 52-μm-thick BNT film exhibits a dielectric constant and a loss tangent of 107 and 0.0006 (Q of 1600) at 1 MHz, respectively. Variation in permittivity is less than 0.02% at a bias voltage ±8 kV/cm. Change of film permittivity with temperature (30–120 °C) is below +58.5 ppm/°C, pointing to a good thermal stability. Preliminary microwave measurements indicate that the losses are not significantly increased up to the gigahertz regime. EPD derived BNT thick films on metallic foils are attractive candidates for microwave communication devices.
 [DOI: 10.1063/1.2435334]

Dielectric materials to be employed as resonators must exhibit high quality factor Q (high Q allows signal distribution or storage with minimum loss), high dielectric constant ε_r (the size of the dielectric resonator is proportional to $1/\varepsilon_r^{1/2}$), small temperature coefficient of resonance frequency (τ_f) (low τ_f avoids drift in frequency due to temperature variations), and good surface finishing.[1,2] Among microwave dielectrics, $BaO–Nd_2O_3–TiO_2$ (BNT) system, and, in particular, 1:1:5 composition, represents an important commercial microwave ceramic family due to its high ε_r (80–90), high Q (1500–4000) at ~3 GHz, and low τ_f (90 ppm/k). [(Refs. 3 and 4) Fuji Titanium Industry Co., Ltd.].

Major trends in the communication industry are towards increased integration, higher frequencies, smaller size, and reduced cost. These trends have reached the point that one can consider the replacement of dielectric components currently utilized in bulk ceramic form, by dielectrics processed as thick films. This approach has the potential advantage of reduced processing costs, and may be applied to resonators, filters, baluns, and antennas. Furthermore, the ability to process thick films conformally on substrates, and also directly on metal foils, opens up the possibility of innovative structures and designs.[5] Thick films are required for most of these applications, rather than thin films, as these are volume devices that store electromagnetic energy within the dielectric volume.

Among thick film production processes electrophoretic deposition (EPD) technology possesses unique advantages.[6,7] EPD has been widely investigated in the fabrication of high-performance functional thick/thin films, such as $(Ba,Sr)TiO_3$, $BaTiO_3$, and $Pb(Zr,Ti)O_3$.[8–10] On the other hand, the fabrication of dielectric films on metal foils is presently of interest for devices integrated into electronic packaging due to cost and space benefits.[11] However, there is no report on the preparation and dielectric properties evaluation of BNT thick films fabricated by EPD on metallic substrates. In this letter, thick films of BNT were prepared by EPD on platinum foils for application in microwave communication devices, and their characterization of electrical properties at rf and gigahertz regime is reported.

BNT thick films were fabricated with commercial BNT (1:1:5) powders [MBRT-90M(B), Fuji Titanium Industry Co., Ltd.]. Powder average particle size was 0.4 μm. Glacial acetic acid was used as solvent media. The concentration of the suspension was 10 g/l. Prior to EPD the suspensions were ultrasonically dispersed and magnetically stirred for 5–10 min followed by settling to sediment coarse particles. The platinum foil as working electrode (cathode) was separated 2 cm from the Pt counterelectrode (anode) in a glass beaker. 12–52-μm-thick BNT films can be deposited by utilizing 40–600 V for 30 s–10 min in glacial acetic acid solvent. The as-deposited films were dried at 90 °C for 24 h. Some green films were then pressed under an isostatic pressure of 200 MPa to enhance the green density. The films were then sintered in air at 1300 °C for 1 h. In order to compare the final properties with those of BNT films, BNT ceramics were prepared. For that, BNT powders (the same as used for film preparation) were pressed under a uniaxial pressure of 20 MPa followed by an isostatic pressure of 200 MPa. The pressed disks were sintered at 1300 °C for 3 h. The structure of the sintered films and ceramics was analyzed by x-ray diffraction (XRD) (Rigaku, Geigerflex D/Max-B). The microstructure of films and ceramics was analyzed by Scanning electron microscopy (SEM) coupled with energy dispersive spectrometer (EDS) (Hitachi, S-4100). The electrical measurements were conducted via a metal-insulator-metal configuration using Au as the top electrode for both films and ceramics. For the case of films, Au top circular electrodes were sputtered using a shadow mask of 0.6 mm diameter. BNT films with top electrode were post-annealed at 200 °C for 30 min to improve the metal/film interface. Au top and bottom 6 mm diameter electrodes were

a)Author to whom correspondence should be addressed; electronic mail: paulas@cv.ua.pt

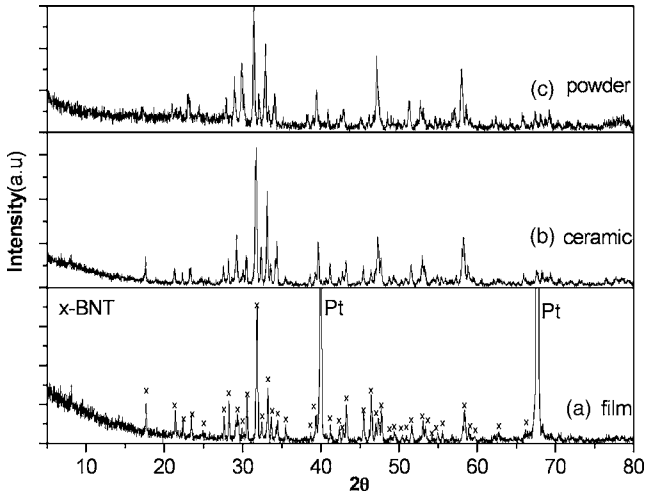

FIG. 1. XRD pattern of (a) BNT sintered thick films, (b) BNT ceramics, and (c) starting BNT powders.

sputtered on 0.8 mm thick ceramics. The electrical properties were evaluated using an impedance bridge (HP 4284A) over a frequency range of 1kHz–1 MHz. The oscillation level of the applied voltage was set to 1.0 V. The analyzed electrical properties include dielectric constant, ε_r, loss tangent, tan δ, temperature dependence of permittivity $(\Delta\varepsilon_r/\varepsilon_{r0}\Delta T)$, and permittivity-voltage variation $(C\text{-}V)$. Preliminary analysis of microwave dielectric properties of BNT thick films was performed. The microwave transmission coefficients S_{ij} were determined by transmission measurements with a network analyzer (HP 8720D) using two separated Au contacts on the thickest BNT film for the rf input and rf output, respectively. The measurement resembles a rf line with two BNT capacitors in series. Modifications of the losses will affect the transmission and reflection. Due to the nonperfect impedance match at the sample only qualitative measurements of the change of the transmission coefficients up to 1.4 GHz were possible.

Figure 1 depicts the XRD patterns of BNT thick films and BNT bulk ceramics sintered at 1300 °C for 1 and 3 h, respectively. Films and ceramics exhibit a well-crystallized phase that corresponds to the orthorhombic structure of $BaNd_2Ti_5O_{14}$ (Ref. 12) with no evidence of preferred orientation or secondary phases for both of them. EDS results demonstrated that no detectable alteration of materials composition occurred for films and bulk ceramics.

The microstructure of green BNT thick films is uniform and homogeneous. The morphology of sintered BNT thick films and bulk ceramics is shown in Fig. 2. BNT ceramics exhibit a dense and homogeneous microstructure with rounded shaped grains [Fig. 2(a)]. However, the microstructure of EPD derived BNT thick films is substantially different from the ceramics one. The films without postdeposition isostatic pressing step exhibit a considerably porous microstructure [Fig. 2(b)] and, identically to the ceramics, the majority of the grains preserve their spherical shape. However, the porosity of these films results in unacceptable dielectric properties. The postdeposition isostatic pressing step proved to be a simple but effective method to achieve dense sintered microstructures. Alternative approaches included increasing the sintering temperatures or introducing liquid phase sintering aids. However, the former approach is not attractive due to the thermal expansion mismatch with the substrate, and in the latter case the sintering aids can easily increase dielectric losses. With the inclusion of the postdeposition isostatic pressing step, sintered BNT films exhibited a very dense microstructure mainly composed of needle shaped grains, as clearly shown in Fig. 2(c). With regard to the origin of elongated grains in BNT thick films, it might arise from the constrained sintering of BNT films on Pt foil due to thermal expansion coefficient differences between BNT films and Pt substrate. Further studies are ongoing to elucidate the mechanism behind the elongated grain growth.

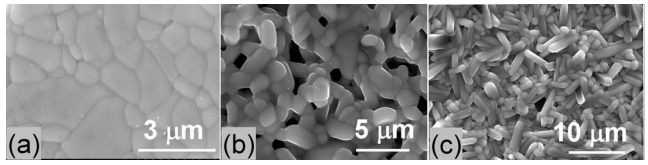

FIG. 2. SEM microstructure of BNT ceramics (a) and BNT thick films without (b) and with isostatic pressing, (c) both sintered at 1300 °C/1 h.

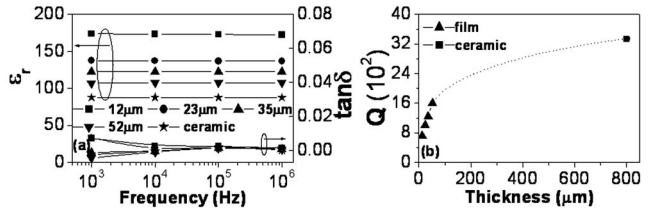

FIG. 3. (a) ε_r and tan δ of BNT films with various thicknesses and ceramics; (b) Q thickness dependence of BNT films and BNT ceramics at 1 MHz. (Dashed line for eye guidance).

ε_r and tan δ of BNT thick films and the effect of film thickness are shown and compared with BNT ceramics in Fig. 3 and Table I. ε_r and tan δ at 1 MHz are 107 and 88 and 0.0006 and 0.0003 for 52-μm-thick-films and ceramics, respectively. As the film thicknesses were increased from 12 to 52 μm, ε_r and tan δ of BNT films approached that of BNT ceramics. Q $(1/\tan\delta)$ values of BNT films with different thicknesses are compared at 1 MHz with bulk ceramic values in Fig. 3(b). As shown, the Q of BNT thick films improved from 700 to 1600 when the film thickness increased from 12 to 52 μm. This trend is consistent with an 'interfacial layer' or interfacial region at the lower foil electrode interface that has lower dielectric constant and slightly increased dielectric loss. As the film thickness increases the macroscopic response of the capacitor tends to be ruled by the bulk of the film and the detrimental influence of the interfacial layer or film defects tends to be minimized. Under the present EPD conditions the film thickness increase above 50 μm will be associated with processing difficulties: increase of deposition time, risk of high voltage induced electrolysis, and film porosity. Besides the influence of the interfacial layer, the lower Q of BNT thick films compared with BNT ceramics might be also related to film microstructure, which have particular grain morphology and some small volume of residual porosity. Meanwhile, compared with other reported microwave thin films, as shown in Table I, the BNT thick films prepared in this work demonstrated an excellent performance in terms of ε_r and tan δ, being the highest Q reported for thick films (>1 μm) so far.

Figure 4 exhibits the temperature dependence of ε_r and applied dc voltage dependences of ε_r and tan δ for BNT thick films, compared with the corresponding ceramics. The

TABLE I. Electric properties of 52-μm-thick BNT films and ceramics sintered at 1300 °C for 1 and 3 h, respectively, and other analog reported materials. (MOD: metal organic deposition; CVD: chemical vapor deposition.)

System	Electrical properties			
	ϵ_r	tan δ and Q	ϵ_r temperature dependence	Reference
BNT films (52 μm)	107	0.0006 or Q=1600 (1 MHz)	+58.5 ppm/°C (30–120 °C)	Current work
BNT ceramics	88	0.0003 or Q=3333 (1 MHz)	−36.8 ppm/°C (30–120 °C)	Current work
BNT ceramics	91	0.0006 or Q=1771 (3.5 GHz)	−8 to −46 ppm/°C (−20–80 °C)	Fuji supplier
$MgTiO_3$ films (300 nm) by MOD	21	0.02 (100 KHz)	···	13
$Ba_{0.7}Sr_{0.3}TiO_3$ films (30 nm) by CVD	80[a]	0.006 (20 GHz)		14
$Ba(Mg_{1/3}Ta_{2/3})O_3$ films (300 nm) by MOD	22.2	0.009 (100 KHz)	−145 ppm/°C (25–125 °C)	15

[a]Capacitance density value fF/μm^2.

temperature dependence of ε_r of BNT film capacitor was analyzed between 30 and 120 °C at 1 MHz. As shown in Fig. 4(a), the dielectric constant is quite stable as a function of temperature for BNT films. The temperature dependence coefficient of ε_r was measured in terms of the parameter $\Delta\varepsilon_r/\varepsilon_{r0}\Delta T$, where $\Delta\varepsilon_r$ stands for the change in ε_r relative to the dielectric constant ε_{r0} at 30 °C. The temperature dependence coefficient of dielectric constant of 52 μm-thick BNT films was calculated to be lower than +58.5 ppm/°C between 30 and 120 °C, indicating a good temperature stability of BNT thick films. Figure 4(b) shows dc electric field dependence of ε_r and tan δ of 52-μm-thick BNT films. The ε_r did not show substantial dependence on the bias voltage, in which variation was found to be less than 0.02% up to an applied voltage of 40 V (8 kV/cm). Preliminary microwave measurements indicated that up to 1.4 GHz no significant increase of the losses takes place in BNT films, i.e., the modification of the internal loss of the film was smaller than the resolution of the experiment of ~0.01 dB for this frequency range. Measurements up to higher frequencies are in preparation.

In summary, high quality BNT thick films were prepared by EPD. It was shown that the density of BNT films can be greatly increased by isostatic pressing treatment after deposition, which resulted in considerable enhancement of the dielectric properties. Dense BNT thick films displayed a homogeneous microstructure with a characteristic needle shape of grain growth when compared with equivalent ceramic samples. Dense BNT thick films exhibit higher ε_r than BNT ceramics prepared from identical starting powders. The dielectric Q is higher than any previously reported for thick films. The excellent dielectric properties, including good thermal stability and bias voltage independent capacitance characteristics, suggest the suitability of EPD BNT thick films for integrated capacitor and microwave device applications.

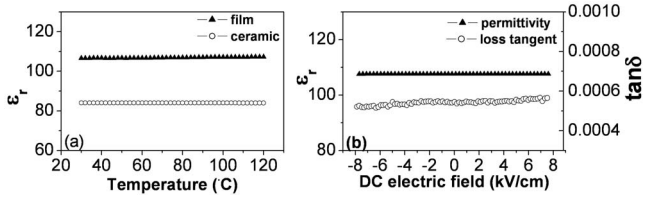

FIG. 4. (a) Temperature dependence of ε_r of 52-μm-thick BNT films and ceramics and (b) dc electric field dependence of ε_r and tan δ of 52-μm-thick BNT films.

One of the authors (Z.F.) acknowledges FCT Portugal for financial support (SFRH/BD/19327/2004). P.V. acknowledges the support of the European Network of Excellence FAME.

[1]Y. B. Xu, Y. Y. He, X. M. Cheng, X. B. Zhang, and L. B. Wang, J. Mater. Sci.: Mater. Electron. **13**, 197 (2002).
[2]R. J. Cava, W. F. Peck, Jr., J. J. Krajewski, G. L. Roberts, B. P. Barber, H. M. O'Bryan, and P. L. Gammel, Appl. Phys. Lett. **70**, 1396 (1997).
[3]D. Kolar, Z. Stadler, S. Gaberscek, and D. Suvorov, Ber. Dtsch. Keram. Ges. **55**, 346 (1978).
[4]R. Uboc, I. M. Reaney, and W. E. Lee, Int. Mater. Rev. **43**, 205 (1998).
[5]H. F. Cheng, Y. C. Chen, and I. N. Lin, J. Appl. Phys. **87**, 479 (2000).
[6]P. Sarkar and P. Nicholson, J. Am. Ceram. Soc. **79**, 1987 (1996).
[7]J. P. Zhang and B. I. Lee, J. Am. Ceram. Soc. **83**, 2417 (2000).
[8]E. Ngo, P. C. Joshi, M. W. Cole, and C. W. Hubbard, Appl. Phys. Lett. **79**, 248 (2001).
[9]J. Van Tassel and C. A. Randall, J. Eur. Ceram. Soc. **19**, 955 (1999).
[10]A. Y. Wu, P. M. Vilarinho, and A. I. Kingon, J. Am. Ceram. Soc. **89**, 575 (2006).
[11]W. J. Borland and S. Ferguson, Circuit Tree (March 2001).
[12]Natl. Bur. Stand. (U.S.) Monogr. 25,19 19 (1982); JCPDS-International Center for Diffraction Data Card No. 33-0166.
[13]Y. H. Choi and J. C. Lww, Thin Solid Films **385**, 43 (2001).
[14]J. D. Baniecki, R. B. Laibowitz, T. M. Shaw, P. R. Duncombe, D. A. Neumayer, D. E. Kotecki, H. Shen, and Q. Y. Ma, Appl. Phys. Lett. **72**, 498 (1998).
[15]P. C. Joshi and S. B. Desu, Appl. Phys. Lett. **73**, 1080 (1998).